Nonlinear Transport Processes in Disordered Media

Muhammad Sahimi
HLRZ Supercomputer Center, c/o KFA Jülich, Postfach 1913, W-5170 Jülich 1, Germany
Dept. of Chemical Engineering, University of Southern California, Los Angeles, CA 90089

Nonlinear transport processes in disordered systems such as porous media and heterogeneous solids are studied, which are represented by two- or three-dimensional networks of interconnected bonds, by a Bethe network (a branching network with no closed loops) of a given coordination number, or by a continuum in which circular or spherical inclusions have been inserted at random. The bonds represent the pores of the pore space, or the conducting and insulating regions of a disordered solid, to which we assign effective properties (radii or conductances) selected at random from a probability density function. Three types of nonlinear transport processes are considered. (1) The relation between the current q and the potential gradient v is of power-law type (as in, for example, flow of power-law fluids or the electric current in doped polycrystalline semiconductors). (2) The relation between q and v is piecewise linear, characterized by a threshold (as in flow of Bingham fluids or in mechanical or dielectric breakdown of composite solids). (3) A large v is imposed on the system, so that a linear transport theory is not valid. The behavioral study of the effective transport and topological properties of the system, such as the permeability, conductivity, diffusivity, and the shape of the sample-spanning cluster of conducting paths shows that in all cases the concepts of percolation theory play a prominent role, even if the system is well connected and percolation may seem not to play any role. For most cases, new effective-medium approximations (EMAs) are derived for estimating effective transport properties. Compared to the case of linear transport, new EMAs are considerably more accurate in predicting the scaling properties of the transport coefficients near a critical point such as the percolation threshold. For a power-law transport process, an exact solution is also derived for the Bethe networks. Using the concepts of percolation theory, scaling laws relating the effective properties to various regimes of transport and to topological properties of the system are also given. A relation between the volumetric flow rate of a power-law fluid in porous media and the macroscopic pressure drop is derived, which contains no adjustable parameter and is valid at any porosity. To test the accuracy of our analytical predictions, Monte Carlo simulations are carried out for several cases. In most cases, good agreement is found between the simulation results and predictions. The extension of the results to other types of nonlinearities is also discussed.

Introduction

The problem of transport in random media is important, in view of its relevance to the modeling of a wide variety of phenomena in natural and industrial processes. A partial list of applications include flow, dispersion and displacement processes in porous media (for a review, see Sahimi, 1993a), diffusion through biological tissues, and transport, mechanical and rheological properties of disordered materials such as pol-

ymers, glasses and powders. In condensed matter physics, such applications include conduction in amorphous semiconductors, frequency-dependent conductivity in superionic conductors, oxygen transport in nuclear reactor fuels, motion of electrons in liquids, and many others.

Most of the transport processes in random media that have been studied so far are *linear*. In practice, there are many natural and industrial processes in which a *nonlinear* transport phenomenon takes place. For example, flow of polymers and other non-Newtonian fluids in a porous medium is a nonlinear process. Brittle fracture and dielectric breakdown of composite solids are two other examples of a nonlinear transport process. In brittle fracture, for example, a disordered solid, which obeys equations of linear elasticity, breaks down and creates microcracks in its structure when the imposed macroscopic stress or strain exceeds a critical threshold (Sahimi and Goddard, 1986; Sahimi and Arbabi, 1992; for a review, see Sahimi, 1992b). In many doped polycrystalline semiconductors, for example, ZnO, the electrical conductivity is highly nonlinear above a threshold voltage. Continuous phase transitions in disordered media, such as the metal-insulator transitions, are usually characterized by the vanishing of some physical quantity of practical relevance and can be accompanied by the shrinkage of the linear-response regime, as the transition point is approached, and the emergence of a nonlinear transport regime. In all of such systems, the interplay between the nonlinear transport process and the disordered structure of the systems gives rise to phenomena that are far more complex than what one usually has to deal with in linear systems.

In this article, we study several different types of nonlinear transport processes in disordered systems such as porous media and composite solids. The disordered system is represented by a network of interconnected bonds. We use two- or three-dimensional networks with a coordination number z, which is the number of bonds connected to the same node or site of the network, or a Bethe network of coordination number z, which is an endlessly-branching structure with no closed loops, an example of which is shown in Figure 1 with $z=3$. In the case of a porous medium, the bonds represent the pores of the pore space. For modeling of disordered solids, the bonds represent the conducting and insulating regions of the system to which are assigned random conductances (including zero conductance to represent the insulating parts). In some cases, this discrete representation of the system may not by suitable, and it may be more appropriate to represent it by a continuum. There are several methods of modeling disordered continua. One can, for example, insert at random circular or spherical inclusions in an otherwise homogeneous medium and obtain the so-called *Swiss-cheese* model (see Figure 2). If the spheres or circles are *not* overlapping, and if transport takes place through the channels *between* the circles or spheres, then the problem can be mapped exactly onto the same transport process on the *edges* of a Voronoi structure (Kerstein, 1983), a 2-D example of which is shown in Figure 3. However, if one uses such a model of a disordered system, one can no longer assign randomly the transport properties of the edges, because there is a *natural* distribution of the conductances which can be constructed based on the particular shapes and sizes that the random channels take on. Such natural distributions can give rise (Feng et al., 1987) to unusual phenomena which cannot be predicted by the network models unless they are used with

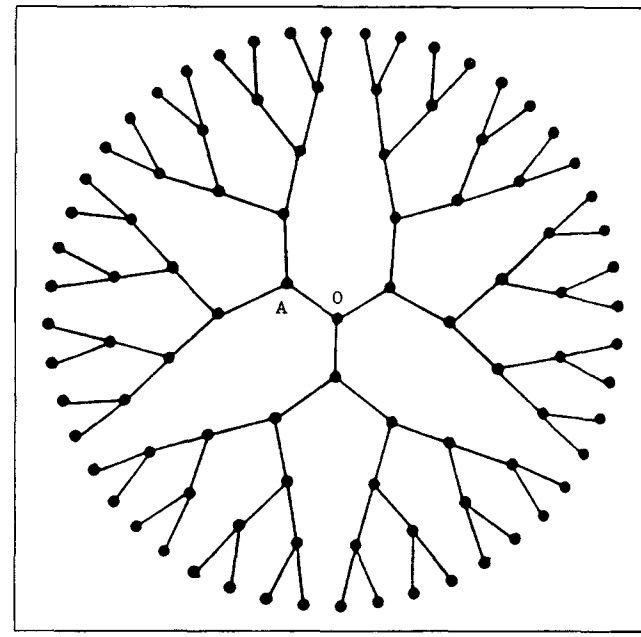

Figure 1. Bethe network of coordination number $z=3$.

the same natural distributions (see below). On the other hand, if in the Voronoi structures one constructs a *dual* network by connecting the centers of the neighboring polyhedra (polygons in two dimensions) to each other, one obtains a Voronoi network (see Figure 3). An efficient and vectorized computer algorithm for generating random networks was developed recently by Moukarzel and Herrmann (1992). In this case too, a natural distribution of the conductances can be constructed.

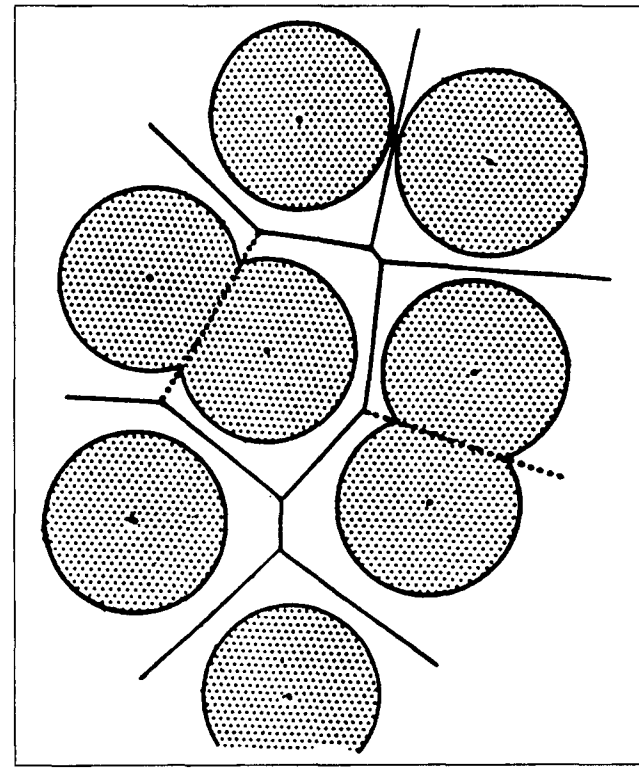

Figure 2. Swiss-cheese model of disordered continua.

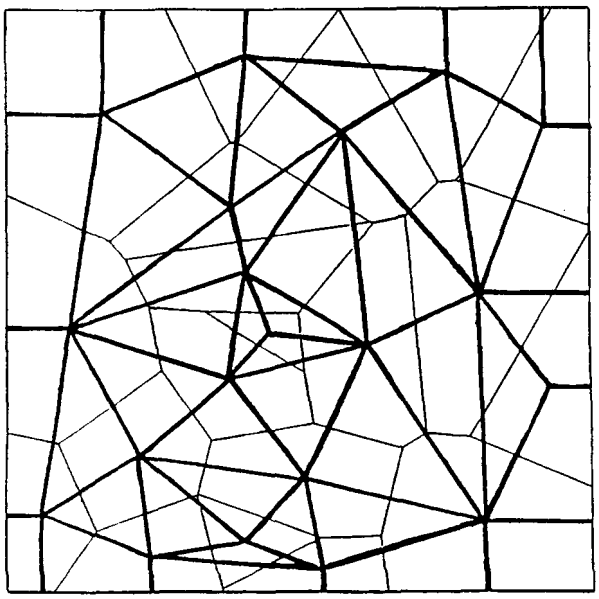

Figure 3. Two-dimensional Voronoi network (thick lines), generated by constructing the dual network of Voronoi tessellation of space.

The average coordination number of the network is 6.

Jerauld et al. (1984) have already shown that as long as the average coordination number of a random network, such as the Voronoi network, and the coordination number of a regular network are equal, the transport properties of the two systems are virtually identical, provided that *the same distribution of the bond conductances is used in both networks*. They did not, however, consider the case of random networks with the natural distributions, nor did they study any nonlinear transport process.

One of the simplest prototypes of a disordered medium is a percolation system. In such a system, a fraction of the bonds (or inclusions in the continuum models) do not allow transport to take place at all. For example, in flowthrough porous media, a fraction of the pores may be closed to the flow of a given fluid, because such pores are occupied by another immiscible fluid or these pores are too small to accommodate the fluid's molecules (see, for example, Sahimi, 1992a). Thus, the interconnectivity of the open pores and the existence of a sample-spanning cluster of such pores play important roles in the overall properties of a transport process in a porous medium. Even in a well-connected system, percolation can play an important role if the distribution of the heterogeneities is *broad*. For example, if the bond conductance distribution of a network is very broad, then a finite fraction of the bonds can take on very small conductances, and hence their contribution to the overall conductivity of the system is very small and can be neglected. Thus, we may set their conductances to be zero and reduce the problem to a percolation process. This idea, which is usually called the *critical path analysis*, was first developed by Ambegaokar et al. (1971) for determining the hopping conductivity of semiconductors and was further developed by Katz and Thompson (1986, 1987) for determining the absolute (single-phase) permeability and electrical conductivity of porous media saturated by a Newtonian fluid. We shall discuss these ideas later by extending them to derive analytical expressions for the effective transport properties of disordered systems in the *nonlinear* regimes.

One of the simplest methods of estimating the effective transport properties of disordered media is the effective-medium approximation (EMA), which is a phenomenological method by which a disordered medium is replaced with a hypothetical homogeneous one with unknown physical constants. In the original EMA developed by Bruggeman (1935) and independently by Landauer (1952) (for a review of the history of EMA, see Landauer, 1978), each inhomogeneity is embedded in the effective medium itself, the unknown properties of which are determined in such a way that the volume average over all inhomogeneities yields no extra field in the medium. Thus, EMA is an ingenious way of transforming a many-body system into a one-body problem. The Bruggeman-Landauer EMA, which was developed for a continuum, was extended by Kirkpatrick (1973) to regular networks of random conductances, and has been shown to be very accurate under a wide variety of conditions. In the chemical engineering literature, such an EMA has been employed by several authors (see, for example, Benzoni and Chang, 1984; Burganos and Sotirchos, 1987; Burganos and Payatakes, 1992; see Sahimi et al., 1990, for a review). The original EMA was developed for steady-state diffusion and conduction processes. Sahimi et al. (1983a) extended them to unsteady-state processes. Moreover, most of various versions of EMA developed so far have been for *linear* transport processes. One major goal of this article is to extend them to *nonlinear* transport processes.

The plan of this article is as follows. In the next section, we discuss briefly the main ideas, concepts and methods of percolation theory and EMA that we shall use in the rest of the article. Next, we treat the three types of nonlinear transport processes mentioned in the abstract of the article, using network models of disordered media. We then discuss how our results can be modified for the continuum models with a natural distribution of the effective properties. The article is summarized in the last section.

Percolation Concepts and the Effective-Medium Approximation

Consider a two- or three-dimensional network of coordination number z, in which a randomly-selected fraction p of the bonds are open to transport (their conductance is nonzero). For convenience we call these the conducting bonds. The rest of the bonds are closed to any transport process (their conductance is zero). As is well-known, if p is small enough no sample-spanning cluster of conducting bonds is formed and macroscopic transport does not exist, whereas for large values of p macroscopic transport does take place. The transition between an insulating and conducting system is characterized by a well-defined value of p, called *the bond percolation threshold* p_c, which depends on z and the dimensionality of the network. In this article, we mostly use the square ($z=4$) and simple-cubic ($z=6$) networks for which, $p_c=1/2$ and 0.249, respectively. For a Bethe network one has, $p_c=1/(z-1)$. One of the most important features of such percolation networks is their *universal* properties near p_c. In this region, one can define a correlation length ξ which diverges as p_c is approached according to the power law

$$\xi \sim (p-p_c)^{-\nu}. \tag{1}$$

The correlation length is the length scale for macroscopic homogeneity of the system. For any length scale $L>>\xi$ the system is macroscopically homogeneous, and thus the classical differential equations of transport with constant transport coefficients are applicable, while for length scales $L<<\xi$ the system is a fractal and statistically self-similar object to which such equations are *not* applicable. The fraction X^A of conducting bonds that are in the sample-spanning cluster vanishes as:

$$X^A \sim (p-p_c)^{\beta}. \tag{2}$$

For any length scale $L<<\xi$, the sample-spanning cluster is a fractal object with a fractal dimension D. To relate D to the other exponents we note that the number of sites (or bonds) N_s in the sample-spanning cluster is $N_s \sim \xi^d X^A \sim \xi^{d-\beta/\nu}$, where d is the Euclidean dimension of the cluster. For $L<<\xi$, we replace ξ by L and obtain $N_s \sim L^{d-\beta/\nu}$. If a fractal dimension D is defined by $N_s \sim L^D$, then we must have:

$$D=d-\frac{\beta}{\nu}. \tag{3}$$

Suppose now that the conductance g of the open bonds is selected randomly from a distribution $f(g)$. Then, the overall conductivity g_m of the network vanishes as p_c is approached according to the power law:

$$g_m \sim (p-p_c)^t. \tag{4}$$

The permeability k of such networks also obeys the same scaling law (Eq. 4). In certain continua, however, there are important differences between the scaling laws for the effective conductivity and permeability. This will be discussed later. The sample-spanning cluster can be divided into two parts: the dead-end part that carries no flow or current, and the *backbone* which is the multiply-connected part of the cluster. Near p_c, the bonds of the backbone are also divided into two groups: the bonds in the *blobs*, which are multiply-connected and make the transport paths very tortuous, and the *red* bonds, which are those that, if cut, would split the backbone into two parts. The reason for calling such bonds red is that they carry all of the current between two blobs, and therefore they are the *hottest* bonds in the cluster (Stanley, 1977). The fraction X^B of the conducting bonds that are in the backbone vanishes as p_c is approached as $X^B \sim (p-p_c)^{\beta_B}$, while for any length scale $L<<\xi$ the backbone is a fractal object with a fractal dimension D_B given by:

$$D_B=d-\frac{\beta_B}{\nu}. \tag{5}$$

Near and at p_c, the number M_{red} of the red bonds in a box of linear size L, with $L<<\xi$, scales with L as $M_{\text{red}} \sim L^{\zeta_{\text{red}}}$, so that ζ_{red} can be interpreted as the fractal dimension of the red bonds. Coniglio (1981) proved that:

$$\zeta_{\text{red}}=1/\nu. \tag{6}$$

On the other hand, for $L<<\xi$, the *resistance* R between two end points of a box of linear size L scales with L as $R \sim L^{\zeta}$. It is easy to show that:

$$t=(d-2)\nu+\zeta, \tag{7}$$

where $\zeta=\tilde{\zeta}\nu$. The interested reader should consult Stauffer and Aharony (1992) for an introduction to percolation theory and Sahimi (1993b) for its various applications. The topological exponents, which describe the connectivity of the sample-spanning cluster and its backbone, are completely universal and depend only on the dimensionality of the system and are the same for percolation in random or regular networks and in continua. For a given transport regime, the exponents t and ζ are also completely universal provided that (Sahimi et al., 1983a):

$$f_{-1}=\int_0^{\infty}\frac{f(g)}{g}\,dg<\infty. \tag{8}$$

Certain continuum models violate the above condition, which is why they should be considered separately. Table 1 presents the currently-accepted values of the critical exponents and the fractal dimensions for 2-D and 3-D networks. Also shown are the same quantities for Bethe networks which, as can be seen, are quite different from those for 3-D networks.

Consider now a *regular* network of coordination number z, and suppose that the conductance of the bonds is selected from a distribution $f(g)$. In an effective medium approach, the random conductances of all bonds are replaced with g_m to create a uniform network. One then replaces, in the uniform network, the effective conductance of one bond with its true value g. This replacement causes fluctuations in the uniform potential distribution in the network. One insists that the average of these fluctuations, when the averaging is taken with respect to $f(g)$, should be zero. This results in a simple equation for g_m which is given by (Kirkpatrick, 1973):

$$\int_0^{\infty}\frac{g_m-g}{g+g_m(z/2-1)}f(g)dg=0. \tag{9}$$

The same method can be used for estimating the effective permeability of a porous medium with random pore permeabilities. If we now choose:

$$f(g)=(1-p)\delta(g)+ph(g), \tag{10}$$

that is, a percolation distribution in which a fraction $1-p$ of the bonds are insulating and the conductances of the rest are selected from a normalized probability density function $h(g)$,

Table 1. Currently-Accepted Values of Critical Exponents and Fractal Dimensions in d-Dimensions*

d	β	ν	β_B	D	D_B	t	$\zeta_{\min}$
2	5/36	4/3	0.48	91/48	1.64	1.3	1.13
3	0.41	0.88	1.05	2.52	1.8	2.0	1.34
Bethe Network	1	1/2	2	4	2	3	2

*Rational or integer numbers represent exact values. For comparison, the corresponding values for Bethe network, which represents the mean-field approximation, are also shown.

then Eq. 9 predicts that g_m vanishes at $p=p_c=2/z$. Thus, this EMA predicts that, $p_c=1/2$ (the exact value) and 1/3 for the square and cubic networks, respectively. It is possible to improve the performance of EMA for the cubic network considerably (Sahimi et al., 1983b). Moreover, if we take, $h(g)=\delta(g-1)$, we find that, $g_m=(p-2/z)/(1-2/z)$, that is, EMA predicts that g_m vanishes *linearly* with $p-p_c$ in both 2-D and 3-D, and so it predicts that $t=1$, which is relatively accurate for 2-D systems, but not so for 3-D ones (see Table 1). However, EMA is very accurate, if p is not very close to p_c. For a disordered continuum with randomly-distributed spherical inclusions, Eq. 9 can still be used if $z/2$ is replaced by $d-1$. Other inclusion shapes can also be considered (see, for example, Thorpe and Sen, 1985), but we do not consider them here.

Power-Law Transport

In this section, we study power-law transport in random networks. We use the analogy between Ohm's law of electrical currents and laminar flow in tubes and use the language of electrical networks, since it simplifies the discussion considerably. Thus, we assume that the relation between current (volumetric flow rate) q and the voltage (pressure) drop v, for any bond (tube or pore), is given by:

$$q=gv^{1/n}, \tag{11}$$

where we interpret g as a generalized conductance. Larson (1981) showed that for slow flow of power-law fluids in a porous medium, *with one injection point and one producing point*, an equation similar to Eq. 11 is also valid for the entire medium. Kenkel and Straley (1982) and Straley and Kenkel (1984) proved the same for *any two-terminal network*. (These are *nontrivial* results.) Thus, although Eq. 11 is a nonlinear relation between q and v at the pore or bond level, its basic form, *with the same power n*, survives at the macroscopic level and is valid for the entire system [of course, for the entire system one has to write, $Q=g_mV^{1/n}$, where Q is the macroscopic current and V macroscopic voltage drop]. The reason for this survival is that power-laws are self-similar, and therefore they preserve their identity under a microscopic-to-macroscopic transformation (that is, power-laws propagate self-similarly). Given this, it is clear that for a random conductance network with power-law conductors the exponent t has to depend on n and, according to Eq. 7, the n-dependence of t has to be through ζ because ν is a topological property which is independent of the transport process. In what follows, we restrict our attention to two-terminal networks, and do not consider multiterminal networks for which it is not even clear that there is a unique relation between Q and V.

Exact Solution on a Bethe Network

To derive an exact solution for the problem on a Bethe network we first need the series-parallel rules for power-law conductors. It is not difficult to show that for N power-law conductors in series or parallel, the equivalent conductivity g_N is given by:

$$g_N=\sum_i g_i, \text{ parallel}, \tag{12}$$

$$g_N=\left(\sum_i \frac{1}{g_i^n}\right)^{-1/n}, \text{ series}. \tag{13}$$

Consider now a Bethe network of coordination number z. The conductance of a branch of the network, starting at the origin O (see Figure 1) can be calculated by simply realizing that it is the equivalent conductance of the bond OA (conductance g_i) in series with the branch that starts at A (conductance G_i). Suppose now that the network is grounded at infinity and that a unit voltage is imposed at O. Then, the total conductance G of the network between O and infinity is that of $(z-1)$ branches which are in parallel. Therefore,

$$G=\left[\sum_{i=1}^{z-1}\left(\frac{1}{g_i^n}+\frac{1}{G_i^n}\right)\right]^{-1/n}. \tag{14}$$

For an infinitely large Bethe network G and G_i are statistically equivalent. Thus, if $H(G)$ is the statistical distribution of G, we must have:

$$H(G)=\int\cdots\int\delta(G-RHS)\prod_{i=1}^{z-1} f(g_i)H(G_i)dg_idG_i, \tag{15}$$

where RHS is the righthand side of Eq. 14. If we take the Laplace transform of Eq. 15 and exploit the fact that all g_i and G_i are randomly and identically distributed, we obtain:

$$\tilde{H}(\lambda)=\left\{\int\int\exp\left[-\lambda\left(\frac{1}{g^n}+\frac{1}{G^n}\right)^{-1/n}\right]\times f(g)H(G)dgdG\right\}^{z-1}, \tag{16}$$

where λ is the Laplace transform variable conjugate to G. For linear flows, $n=1$, Eq. 16 reduces to the equation that was derived by Heinrichs and Kumar (1975). For this limit a closely-related equation was also derived by Stinchcombe (1974). At this point we can calculate *two* different conductivities for the network. The first conductivity, g_f, is obtained if we ground the Bethe network at infinity and impose a unit voltage at O, and define the conductivity to be the current that flows out along one of the outgoing bonds. The second conductivity, g_s, which is also what one usually calculates for 2-D or 3-D networks, is the average current density per unit applied field. The difference between the two cases is in the geometry of the applied field and the boundary conditions at infinity (see Straley, 1977, for more discussion of this point). The peculiar nature of Bethe networks gives rise to important differences between the two quantities. For example, for linear flows ($n=1$) near p_c one has:

$$g_f\sim(p-p_c)^2, \tag{17}$$

$$g_s\sim(p-p_c)^3. \tag{18}$$

However, observe that Eq. 17 has the same form as that of 3-D networks (for which $t\simeq 2$; see Table 1), whereas Eq. 18 is distinctly different from the conductivity scaling law for 3-D networks. Heiba et al. (1982) proposed g_f as an accurate ap-

proximation to the conductivity of 3-D networks, and this idea has been used by several authors, especially in the chemical engineering literature (see Sahimi et al., 1990, for a review). Since Eq. 17 is similar to the scaling law for 3-D networks, and because by varying z the percolation threshold of a Bethe network can be adjusted to match that of a 3-D network, it is clear that for linear transport g_f can provide an excellent approximation to the conductivity of 3-D networks. For this reason, many authors have claimed that a Bethe network can actually represent a 3-D random conductance network. However, this claim has no theoretical justification. It just happens that, by a happy coincidence, Eq. 17 is similar to that of 3-D networks. Many other properties of Bethe networks are distinctly different from those of 3-D networks, the best example of which is given in Table 1 where we list the values of various exponents. For the present nonlinear case, we use g_f as an approximation to that of 3-D networks (that is, we assume that $g_m \simeq g_f$), keeping in mind the subtle difference between the two quantities. It is then straightforward to show that this conductivity, which we now denote by g_m, is essentially the average of the distribution $H(G)$ and is given by, $g_m = z\langle G\rangle/(z-1)$. Using the properties of the Laplace transforms, it is not difficult to show that g_m is given by:

$$g_m = z\left\{\int\int f(g)H(G)\left(\frac{1}{g^n}+\frac{1}{G^n}\right)^{-1/n} dg dG\right\}^{z-2}, \quad (19)$$

which reduces to the equation given by Stinchcombe (1974) and Heinrichs and Kumar (1975) in the $n=1$ limit. Thus, the procedure to calculate g_m is to first solve the nonlinear integral equation (Eq. 16) for $H(G)$, and use the solution in Eq. 19 to calculate g_m. Both Heinrichs and Kumar (1975) and Stinchcombe (1974) described numerical and analytical techniques for solving such equations in the limit $n=1$. The method of Heinrichs and Kumar is suitable for analyzing the problem near p_c, while Stinchcombe's method is more efficient for $p>>p_c$. We used both of these methods for calculating g_m.

We now use Eqs. 16 and 19 to investigate the behavior of g_m near p_c. If distribution function (Eq. 10) is used in Eqs. 16 and 19, it will not be difficult to show that:

$$g_m = \frac{2c(z-1)^{2+1/n}}{h_n^{1/n}(z-2)}\left[\frac{1}{(z-1)^n-1}\right]^{1/n} [n\Gamma(J-n-1)]^{1/n}\left(p-\frac{1}{z-1}\right)^{1+\frac{1}{n}}, \quad (20)$$

where c is a constant of order unity, Γ is the Gamma function, $J=2+[n]$, where $[n]$ denotes the integer part of n, and

$$h_n = \int_0^\infty \frac{h(g)}{g^n}\, dg. \quad (21)$$

For example, for most polymeric liquids that can be modeled as a power-law fluid, $n<1$, $[n]=0$, and therefore, $J=2$. Equation 21 tells us that $h(g)$ has to have finite inverse nth moments (Eq. 21) in order for g_m to obey scaling law (Eq. 20). Note that Eq. 20 reduces to Eq. 17 in the limit $n=1$. Note also that, had we calculated g_s, the corresponding exponent in Eq. 20 would have been $(5+1/n)/2$ (Straley and Kenkel, 1984), and the prefactor c would have also been quite different, which is another indication of the large difference between g_f and g_s.

Scaling and Critical Path Analyses

In this subsection, we provide a scaling analysis of power-law transport in random conductance networks, and study the dependence of the exponent $t(n)$ on n. This will then be used in conjunction with an extension of the critical path analyses of Ambegaokar et al. (1971) and Katz and Thompson (1986, 1987) to derive an expression relating the volumetric flow rate of a power-law fluid in flow through porous media to the macroscopic pressure drop ΔP. To being with, scaling law (Eq. 7) has to be generalized to the case of power-law transport. This has already been done by Kenkel and Straley (1982) who showed that:

$$t_n = t(n) = (d-1)\nu + \frac{\zeta(n)-\nu}{n}, \quad (22)$$

where ζ is now a function of n. In general, t_n is larger than t, and therefore the conductivity curve for power-law transport near p_c is flatter than that of the linear transport regime. We now relate $\zeta(n)$ to the *topological* exponents of percolation networks defined above. This will allow us to see how $\zeta(n)$ varies with n. It can be proven that:

$$\tilde{\zeta}(n=\infty) = \zeta_{\text{red}}. \quad (23)$$

To prove this, consider a two-terminal blob of bonds near p_c, and suppose that the current through the blob is Q, while the voltage between its two terminals is V. Thus, the resistance R of the blob is given by, $R = V^{1/n}/Q$. Now, if we select any transport path between the two ends of the blob, we can write, $V = \Sigma_i r_i q_i^n$, where r_i is the resistance of bond i along the path, and q_i its current. Therefore,

$$R = \left[\sum_i r_i\left(\frac{q_i}{Q}\right)^n\right]^{1/n}. \quad (24)$$

However, $q_i<Q$, and, therefore, $(q_i/Q)^n$ should vanish as $n\to\infty$, which implies that the blob resistance will be zero. This means that the blob does not offer any resistance to the transport, and thus all of the resistance is offered by the red bonds. This proves Eq. 23 [which was first given by Blumenfeld and Aharony (1985) who studied power-law transport in two simple fractal structures]. Another relation between $\zeta(n)$ and a topological exponent can be obtained by straightforward manipulation of the network properties. If we calculate the dissipated power I in a network, we obtain:

$$I = \frac{|Q|^{n+1}}{G} = \sum_i r_i |q_i|^{n+1}. \quad (25)$$

Hence, if we set $n=-1$ in Eq. 25, we obtain:

$$R = \frac{1}{G} = \sum_i r_i. \quad (26)$$

If the bond conductances r_i are all unity, then Eq. 26 implies that the resistance is simply the sum of all current-carrying bonds of the network, which are in the backbone, as described earlier. In view of Eq. 5 we conclude that:

$$\tilde{\zeta}(n=-1)=D_B. \tag{27}$$

This result was first given by Blumenfeld et al. (1986). Thus, although the limit $n=-1$ may not seem physical to an engineer, it provides a connection between the properties of a nonlinear transport process and a purely topological property of the disordered medium. Using the values of the various exponents given in Table 1, we see that in 2-D, $\zeta(n=\infty)=1$, and $\zeta(n=-1)\simeq 2.18$, whereas $\zeta(n=\infty)=1$, and $\zeta(n=-1)\simeq 1.6$ in 3-D. Therefore, $\zeta(n)$ is a slowly-varying function of n. Meir et al. (1986) calculated $\zeta(n)$ numerically for many values of n. Using their results, we present in Figure 4 the variations of $t(n)$ with n. Note that, it has not been possible to relate $\zeta(n=1)$ to the topological exponents. This indicates the richness and interesting features of power-law transport in random media. Having calculated $t(n)$, we can now turn our attention to a critical path analysis of power-law transport in random media.

The essence of the critical path analysis is as follows. One argues that transport in a heterogeneous medium with a *broad* distribution of conductances is dominated by those conductances whose magnitudes are larger than some characteristic value g_c, which is the smallest conductance such that the set of conductances $\{g_p | g_p > g_c\}$ forms a conducting sample-spanning cluster. Therefore, transport in a disordered medium with a broad conductance distribution reduces to a percolation problem with a threshold conductance g_c. This means that we can set the conductances of all bonds whose magnitudes are less than g_c to be zero, since the contribution of such bonds to the macroscopic conductivity is very small. Doing this reduces the problem to a percolation process near the percolation threshold p_c. Thus, one has a trial solution for the conductance of the sample which is of the following form:

$$g_m = a_1 g_c [p(g_c) - p]^t, \tag{28}$$

which is just the scaling law of the conductivity, Eq. 4. Here, $p(g_c)$ denotes the probability that a given conductance is greater than or equal to g_c, and a_1 is a constant. Equation 28 is then maximized with respect to g_c to obtain $p(g_c)$.

Katz and Thompson (1986, 1987) extended these ideas to estimate the permeability and electrical conductivity (and, hence, the diffusivity) of porous media saturated by a Newtonian fluid. In a porous medium the local hydraulic conductance is a function of the length l. Therefore, the critical conductance g_c defines a characteristic length l_c. Since both flow and electrical conduction belong to the class of scalar percolation problems, the length that signals the percolation threshold in the flow problem also defines the threshold in the electrical conduction problem. Thus, we rewrite Eq. 28 as:

$$g_m = \phi g_c(l)[p(l) - p_c]^t, \tag{29}$$

where the porosity ϕ ensures a proper normalization of the fluid, and g_c is equal to $c_f l^3$ for the flow problem, where the constant c_f is obtained by solving the flow problem in a single pore (or tube). For appropriate choices of the function $p(l)$, the conductance $g_c(l)$ achieves a maximum for some $l_{\max} \le l$.

If $p(l)$ allows for a maximum in the conductance, if the maximum occurs for $l_{\max} \le l$, and if the pore size distribution of the pore space is very broad, then Katz and Thompson obtained

$$l_{\max} \simeq \frac{1}{1+t} l_c, \tag{30}$$

so that with $t \simeq 2$ for 3-D systems, one obtains, $l_{\max} \simeq l_c/3$ for linear flows ($n=1$). The permeability k of the system is now written as:

$$k = a_2 \phi (l_{\max})^2 [p(l_{\max}) - p_c]^t, \tag{31}$$

where a_2 is a constant. To obtain the constant a_2, Katz and Thompson assumed that at a local level the rock conductivity is g_0, the conductivity of the fluid that saturates the pore space, and that the local pore geometry is cylindrical. This immediately implies that, $a_2 = 1/32$ (which is obtained from the solution of laminar flow in a cylindrical tube), and leads to the following expression

$$k_{KT} = \frac{l_c^2}{226F}, \tag{32}$$

where $F = g_0/g_m$ is the formation factor of the rock, and is a measure of the tortuosity of the medium. Equation 32 contains no adjustable parameter: every parameter is precisely defined. To obtain the characteristic length l_c, Katz and Thompson proposed to use mercury porosimetry, which is a percolation process. In a typical mercury porosimetry experiment, the pore

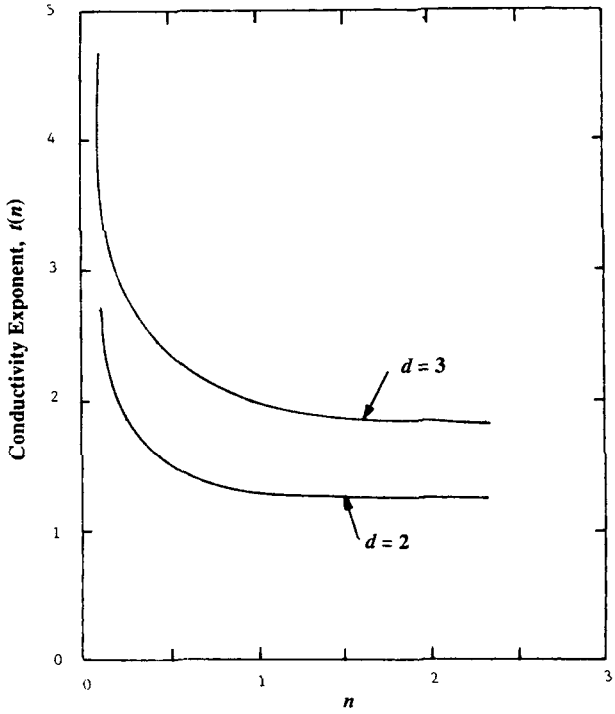

Figure 4. Variations of power-law conductivity exponent $t(n)$ with n.

volume of the injected mercury is obtained as a function of the applied pressure. Normally, in the initial portion of the curve the curvature is positive. This portion is obtained *before* a sample-spanning cluster of pores, filled with mercury, has been formed. After this initial portion, one arrives at an inflection point beyond which the pore volume increases rapidly with pressure. This inflection point signals the formation of a sample-spanning cluster. Therefore, from the Washburn equation we must have $l \geq -4\sigma_s \cos\theta / P_i$, where σ_s is the surface tension, θ the contact angle, and P_i the pressure at the inflection point. Hence, $l_c = -4\sigma_s \cos\theta / P_i$ defines the characteristic length l_c and can be obtained from a routine mercury porosimetry experiment. Equation 32 has been shown to be highly accurate for a wide variety of porous media over the entire range of porosity (see Sahimi, 1993a, for a review).

We can use the same ideas to derive an expression relating Q to ΔP for flow of a power-law fluid in porous media. What we need is the solution to the problem of flow of a power-law fluid in a cylindrical tube, so that we can relate the flow conductances to the length l (through $g \sim c_f l^3$; see above), and the relation between $t(n)$ and n. The latter is given by Eq. 22 and Figure 4. For the flow of a power-law fluid in a cylindrical tube we have $q = g(\Delta p)^{1/n}$, where q is the volumetric flow rate, Δp the pressure drop along the tube, and (see, for example, Bird et al., 1987):

$$g = \frac{n\pi}{1+3n}\left(\frac{1}{2m}\right)^{1/n} l^3, \tag{33}$$

where m is the usual parameter of a power-law fluid. Equation 30 can still be used, except that one should replace t with $t_n = t(n)$. Thus, repeating the procedure of Katz and Thompson (1986, 1987) for the present problem, we find that for flow of a power-law fluid through a porous medium, the macroscopic flow rate Q is related to the macroscopic pressure drop ΔP through the following relation

$$Q = \left(\frac{C_n}{m}\right)^{1/n} (k_{KT})^{\frac{n+1}{2n}} \left(\frac{\Delta P}{L}\right)^{1/n}. \tag{34}$$

where k_{KT} is the permeability of the medium for linear flow problems (Eq. 32), and L the length of the medium. The constant C_n is given by:

$$C_n = \frac{(7.8)^{1-n}(23.6t_n)^{t_n}}{2^{2n+1}(1+3n)^n(1+t_n)^{2+t_n}} F^{2(1-n)/5} \phi^{(n-1)/10}. \tag{35}$$

Equation 34 can be considered as a generalization of Darcy's law for flow of a power-law fluid in a porous medium. Equation 35 can be simplified further since Katz and Thompson (1987) related F to the porosity of the system by:

$$\frac{1}{F} = \frac{l_{\max}}{l_c} \phi S(l_{\max}), \tag{36}$$

where $S(l_{\max})$ is the volume fraction of connected pores involving pore widths of size $l_{\max}$. It is clear that if one specifies the parameters n and m of a power-law fluid and carries out a mercury porosimetry experiment to estimate l_c (and thus k_{KT}), then all parameters of Eqs. 34 and 35 are completely specified, and no adjustable parameters need to be used. Unfortunately the available experimental data on polymer flow in porous media do not contain the capillary pressure curves of the media. Hence, we cannot estimate l_c for such porous media, and therefore we are unable to evaluate the performance of Eqs. 34 and 35. Note that, neither Eq. 32 nor Eq. 34 is exact, because the critical path analysis, based on which these equations were derived, is not exact. But the success of Eq. 32 in predicting the experimental data for permeability of various porous media for Newtonian fluids indicates that the critical path analysis provides an excellent approximation to the problem. Based on this success, we believe that Eqs. 34 and 35 would also provide a highly accurate relation between Q and ΔP for power-law fluids in porous media.

Over the years, many authors have investigated flow of polymers through a porous medium, and have used power-law constitutive equations to correlate their experimental data. Some of these works include those of Christopher and Middleman (1965), Marshall and Metzner (1967), Gogarty (1967), Savins (1969), Hirasaki and Pope (1974), Sheffield and Metzner (1976), Odeh and Yang (1979), Teeuw and Hesselink (1980), Chauveteau and Zaitoun (1981), Duda et al. (1983), and Wu et al. (1991). Almost all of the previous theoretical studies used the bundle of parallel capillary tubes as the model of the porous medium, based on which various expressions relating Q and ΔP were derived. For example, Teeuw and Hesselink (1980) proposed an expression similar to Eq. 34 in which, instead of our k_{KT}, they used the absolute permeability of the porous medium which was estimated by using the bundle of capillary tube model (see Scheidegger, 1974). The coefficient C_n of their expression is given by:

$$C_n = 2^{(3n+1)/2}\left(\frac{n}{3n+1}\right)^n \phi^{(n-1)/2}. \tag{37}$$

Christopher and Middleman (1965) also presented an equation similar to that of Teeuw and Hesselink (1980), except that their C_n is given by:

$$C_n = 150^{(n-1)/2} \frac{4}{3^{n-1}} \left(\frac{n}{3n+1}\right)^n \phi^{(n-1)/2}. \tag{38}$$

A similar equation was used by Hirasaki and Pope (1974). Note that the ϕ-dependence of Eq. 35 is weaker than that of Eq. 37 or 38. Sheffield and Metzner (1976) criticized such correlations, and stated correctly that a bundle of capillary tubes cannot take into account the effect of the 3-D nature of a porous medium, which they showed was essential for flow of polymers in porous media. Instead, they used a constricted unit cell model in which the pores do not have equal size mouths. Their model, although more realistic than the bundle of capillary tube model, cannot also take into account the effects for which Sheffield and Metzner criticized others. We believe that Eqs. 34 and 35 offer a viable alternative to all the expressions that had been developed previously based on the bundle of capillary tube and similar models.

Effective-Medium Approximation

In this subsection, we derive an EMA for power-law transport processes through networks of random conductances. To

begin with, let us first derive an EMA for the Bethe networks. To do this, we follow the method developed by Stinchcombe (1974) and Heinrichs and Kumar (1975). The basic idea is to assume that the statistical distribution of the conductance G is of the form, $H(G)=\delta(G-G_m)$, where G_m is the mean value of G, and to derive a power-series solution for Eq. 19 in the limit of large z. As Stinchombe (1974) and Heinrichs and Kumar (1975) showed, the first term of the power-series solution is equivalent to an EMA for Bethe networks. We do not give the details of our derivation here since it is a direct extension of their works, although the algebra for the present problem is more complex than the linear case studied by them. Using their method, an EMA for a Bethe network of coordination number z is found to be:

$$\int_0^\infty \left\{\frac{(z-1)g}{[g^n+((z-1)^n-1)G_m^n]^{1/n}}-1\right\}f(g)dg=0, \tag{39}$$

and the effective conductivity g_m of the network is given by, $g_m=zG_m/(z-1)$. In the limit $n=1$, Eq. 39 reduces to:

$$\int_0^\infty \frac{g-G_m}{g+(z-2)G_m}f(g)dg=0, \tag{40}$$

which was given by Stinchcombe (1974) and Heinrichs and Kumar (1975).

We now present two different EMAs for 2-D or 3-D networks. The first EMA is obtained by comparing Eqs. 40 and 9. As can be seen, the only difference between the two equations is in the coefficients of g_m in the denominators of the two equations. If in Eq. 40 we replace $(z-2)$ with $(z/2-1)$, we obtain Eq. 9. That is, the role of $(z-2)$ in Eq. 40 is played by $(z/2-1)$ in Eq. 9. Thus, assuming that the same is true for power-law transport, which is a reasonable assumption given that z is a topological property, Eq. 39 can be converted into an EMA for 2-D or 3-D networks of coordination number z. The result is given by:

$$\int_0^\infty \left\{\frac{gz/2}{[g^n+((z/2)^n-1)g_m^n]^{1/n}}-1\right\}f(g)dg=0, \tag{41}$$

which reduces to Eq. 9 in the limit $n=1$. The second EMA was derived by Bernasconi and Tua (1989) for a 2-D continuum with circular inclusions which we extend here to networks of random conductances with coordination number z. One first defines a *tangent* or *differential* conductance σ by:

$$\sigma=\frac{dq}{dv}, \tag{42}$$

which, for the case of linear transport, yields the usual $\sigma=g$. Equation 42, when combined with Eq. 11, yields:

$$\sigma=\frac{g}{n}v^{(1-n)/n}. \tag{43}$$

Consider now a two-phase system which is characterized by tangent conductances σ_1 and σ_2, and keep in mind that they both depend on the voltage v. Recall that in the EMA approach one inserts in the effective medium a bond with its true conductance, and determines the voltage along this bond, that is, the voltage in the effective medium plus the fluctuation that is caused by the insertion of the bond with its true conductance. Carrying this out for the phase $i(i=1,2)$ yields:

$$v_i=\frac{\sigma_m(v_1,\,v_2)z/2}{\sigma_i(v_i)+\sigma_m(z/2-1)}v_m, \tag{44}$$

where v_m is the voltage along the bond in the effective medium, and σ_m is the effective value of σ. If we now apply the usual idea of an EMA, namely, that the average of v_i must be equal to v_m (or the average of the fluctuations must be zero), we obtain:

$$\int_0^\infty \frac{\sigma_i(v_i)-\sigma_m}{\sigma_i+\sigma_m(z/2-1)}f(\sigma_i)d\sigma_i=0, \tag{45}$$

which is the same as Eq. 9 except that the conductances σ_i and σ_m are functions of the voltage. If our system is made of two phases with volume fractions p and $(1-p)$, then

$$pv_1+(1-p)v_2=v_m. \tag{46}$$

The generalization of Eq. 46 to a N-phase system is obvious. The last two equations can be used to determine σ_m. Having determined this quantity, we can calculate g_m using Eq. 43.

To compare the two EMAs, let us consider a simple case. We use distribution (Eq. 10) with $h(g)=\delta(g-1)$, that is, the case in which a fraction $(1-p)$ of the bonds have $g=0$, while the rest take on $g=1$. In this limit, Eq. 41 reduces to:

$$g_m=\left[\frac{(pz/2)^n-1}{(z/2)^n-1}\right]^{1/n}, \tag{47}$$

while the second EMA predicts that:

$$g_m=p^{(n^2-1)/n}\left(\frac{p-2/z}{1-2/z}\right)^{1/n}. \tag{48}$$

We can now compare these formulae in a few limiting cases, and also test their validity. First of all, they should reduce to the linear case for $n=1$, which they both do. Secondly, the percolation threshold that they predict should be the same as in the case of linear transport, since p_c is a topological property and should not depend on the transport regime. Both equations predict that g_m vanishes at $p=p_c=2/z$, the same as in the case of linear transport. Thirdly, both equations predict that, $t_n=1/n$, which is not correct. For example, for 2-D networks and $n=1/2$, Eqs. 47 and 48 predict that $t_n=2$, whereas the numerical estimate (see Figure 4) is $t_n\sim 1.46$, which means that the EMAs prediction is in error by about 37%. However, for 3-D networks and $n=1/2$, the two EMAs still predict that, $t_n=2$, whereas Figure 4 gives, $t_n\simeq 2.35$, that is, the EMA's prediction is about 17% in error. Therefore, as far as the power-law conductivity exponent is concerned, the performance of the EMA *improves* as the dimensionality of the system increases. On the other hand, observe that in the case of linear transport and for the same 2-D and 3-D networks, EMA predicts that, $t=1$, whereas the actual values are (Table 1) $t\simeq 1.3$

and 2, respectively: the EMA performance *worsens* as the dimensionality of the system increases, and in fact the 3-D prediction is in error by a factor of 2. Therefore, compared with the linear case, the predictions of our EMAs improves for the power-law conductivity exponent considerably, and the improvement is particularly dramatic in three dimensions.

We can also compare these with the prediction of Bethe networks, Eq. 20. If we use this equation we find that for $n=1/2$ we have, $t_n=1+1/n=3$, which is about 28% in error when compared with the 3-D case. Hence, compared with the linear case, the performance of Bethe networks, as an approximation to 3-D systems, also becomes poorer. This again demonstrates the richness and interesting features of power-law transport in random media. We should point out that, based on heuristic arguments, Cannella et al. (1988) proposed the following EMA for 2-D and 3-D networks:

$$\int_0^\infty \left[\left(\frac{g_m z/2}{g+(z/2-1)g_m} \right)^n - 1 \right] f(g)dg = 0. \tag{49}$$

However, although this equation does reduce to Eq. 9 in the limit $n=1$, some of its predictions are unphysical. For example, it predicts that g_m vanishes at, $p=p_c=1-[(z-2)/z]^n$, which implies that p_c depends on the transport regime and the value of n, which is not physical. Therefore, we do not believe that Eq. 49 represents a valid EMA for power-law transport through random media.

Monte Carlo Simulation of Power-Law Transport

We should first point out that given a pore size distribution $r(R_t)$ one can, with the aid of a network model of porous media and Monte Carlo simulations, or the EMAs discussed here, calculate rheological properties of a power-law fluid in flow through porous media. Consider, as an example, the calculations of the apparent viscosity μ_a, a quantity that is frequently calculated in the polymer literature (Bird et al., 1987). For flow of a power-law fluid through a cylindrical tube we have, $q=g(\Delta p/l)^{1/n}$, where l is the length of the tube, and

$$g=\frac{\pi n R_t^{3+1/n}}{(3n+1)(2m)^{1/n}}, \tag{50}$$

where R_t is the radius of the tube, and m the usual parameter of a power-law fluid (cf. Eq. 33 in which it has been assumed that $l=R_t$, which is the standard assumption in the critical path analysis). Thus, given a $r(R_t)$ we can calculate $f(g)$ since, $f(g)=(dR_t/dg)r(R_t)$. We can then use this $f(g)$ with an EMA to calculate g_m, the effective volumetric flow rate, $Q_m=g_m(\Delta P/L)^{1/n}$, where L is the length of the medium, and therefore a Darcy velocity $u_m=(\phi Q_m)/S$, in which S is the cross-sectional area of the porous medium. On the other hand, as we pointed out above, we can also use the same EMA to calculate the effective permeability k of the medium by converting $r(R_t)$ into a permeability distribution (since the tube permeability is proportional to R_t^2). Having determined u_m and k, we can calculate an apparent viscosity μ_a for the power-law fluid using, for example the relation, $\mu_a=(k\Delta P)/(Lu_m)$. Of course, any other definition of μ_a can also be used (see, for example, Bird et al., 1987). Similar methods can also be used for other rheological properties of the power-law fluid such as the apparent shear rate (Sorbie et al., 1989). The advantage of such a method is that the effects of pore space dimensionality, pore size distribution, coordination number, and the tortuosity can be automatically taken into account. Therefore, calculating g_m (or k) effectively allows us to determine *all* quantities of interest. For this reason, we only focus on Monte Carlo calculation of g_m and the comparison of the results with the predictions of our EMAs.

We carried out Monte Carlo simulations to calculate g_m, using a $L\times L$ square network and a $L\times L\times L$ cubic network, where L is the number of nodes in a given direction. We used $L=250$ and 15 for the square and cubic networks, respectively. A fixed potential gradient was imposed in one direction of the networks, and periodic boundary conditions were used in the other directions to reduce the effect of finite size of the networks. In the case of the square network one has to solve 62,000 nonlinear equations, while for the cubic network the number of equations to be solved is 2,929. All equations for nodal potentials were solved using a Newton-Raphson method, and the solution for each value of p was used as the initial guess for a smaller value of p. We also averaged the results over ten different realizations of each network. Although any conductance distribution can be used, we restrict our attention to a percolation distribution, Eq. 10, with $h(g)=\delta(g-1)$. Although this distribution may seem too simple, it provides in fact the most stringent test of our analytical predictions, since it is usually with percolation distributions that approximate theories such as an EMA breakdown (see, for example, Koplik, 1981). We restrict our attention to $n<1$, which is the regime of interest to flow of polymers.

Figure 5 compares our Monte Carlo results in the square network for $n=1/2$ with the predictions of Eqs. 47 and 48. Values of $g_m(p)$ have been normalized with $g_m(1)$. Our numerical results for $n=1/2$ are consistent with, but presumably

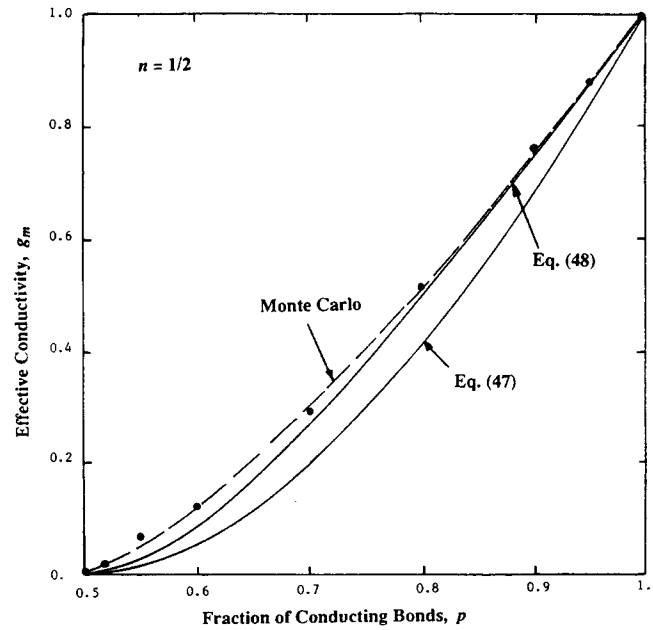

Figure 5. Comparison of Monte Carlo results with the predictions of the EMAs for the square network.

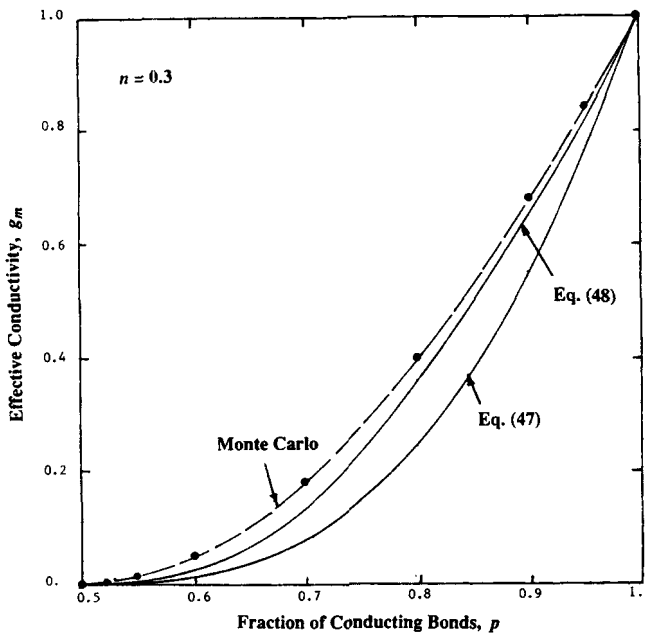

Figure 6. Comparison of Monte Carlo results with the predictions of the EMAs for the square network.

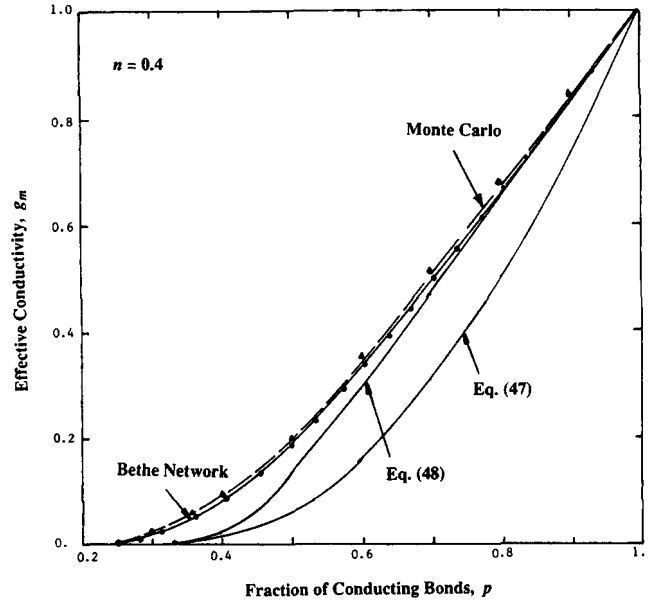

Figure 7. Comparison of Monte Carlo results with the predictions of the EMAs and a Bethe network of coordination number $z=5$ for the cubic network.

more accurate than, those of Tua and Bernasconi (1988) who used smaller square networks, and also employed insulating boundary conditions on the sides of the network parallel to the macroscopic potential drop. Such boundary conditions do not usually eliminate the effect of finite size of the network (Tua and Bernasconi studied only the $n=1/2$ case in the square network). For $p \geq 0.75$, the agreement between the numerical results and the predictions of Eq. 48 is excellent, and the predictions of the two EMAs differ by about 15%. Figure 6 compares the results for the square network for $n=0.3$, and the same trends as those in Figure 5 are also found here. In general, for $0.5<p<0.75$, Eq. 48 is more accurate than Eq. 47. Figure 7 compares the Monte Carlo results in the cubic network for $n=0.4$. In this case, we cannot expect the two EMAs to perform well in the entire range of p, since they do not predict the correct percolation threshold. However, for $p \geq 0.5$ the predictions of Eq. 48 follow closely the Monte Carlo results, while those of Eq. 47 are not in good agreement with the Monte Carlo results. In general, Eq. 48 is more accurate than Eq. 47 in both 2-D and 3-D, especially for small values of n. This is due to the $p^{(n^2-1)/n}$ factor that forces Eq. 48 to predict larger values of g_m than those predicted by Eq. 47. We also present in Figure 7 the predictions of the Bethe network model, Eqs. 16 and 19, where we used $z=5$ so that the percolation threshold of the network, $p_c=1/4$, would closely match that of the cubic network, $p_c \simeq 0.249$. As can be seen, the predictions of the Bethe network model are in good agreement with the Monte Carlo results. Moreover, in contrast with Eqs. 47 and 48, the Bethe network solution has the advantage of providing accurate predictions for the range, $0.25<p<0.33$, where the two EMAs fail completely. However, it is very difficult to obtain the numerical solution of Eqs. 16 and 19, especially for $n<1$, even when one uses a simple percolation distribution, whereas it is straightforward to solve the EMA equation with any $f(g)$. On the other hand, one can improve the predictions of the EMA by combining it with a position-space renormalization group method (Sahimi et al., 1983b). For example, this hybrid method would predict $p_c \simeq 0.265$ for the cubic network, much closer to the true value, $p_c \simeq 0.249$, than the EMA prediction, $p_c=1/3$. The success of this hybrid method in predicting linear transport properties of 3-D disordered systems has been documented elsewhere (Sahimi, 1988), and therefore will not be discussed any further.

Piecewise Linear Transport Characterized by a Threshold

We now consider transport processes that are piecewise linear and are characterized by at least one threshold. Of course, any piecewise linear transport is in fact a highly nonlinear process. In many cases, the regime below the threshold is degenerate in the sense that nothing interesting can happen if the driving force of the system is below its threshold value. For example, Bingham fluids are viscous if the shear stress is larger than a critical value τ_c, but do not flow if the stress is less than τ_c. Foams, which are generally considered as non-Newtonian fluids, are used in displacement and enhanced oil recovery processes for increasing the mobility of the displacing fluid and stabilizing the process. However, to mobilize the foam in any pore, the applied pressure has to exceed a critical value p_{cr}, otherwise the foam will not flow. In brittle fracture, no microcrack nucleation takes place unless the applied stress or strain exceeds a critical value which depends on the size of the system (Arbabi and Sahimi, 1990). Bipolar Zener diodes (which are commercially called varistors) switch from being a nonconducting link to a conducting one at an onset voltage threshold v_c. More generally, a network of such diodes can become conducting if the voltage applied to the system is larger than a critical value V_c. In granular materials, *contacts* between

particles have asymmetric characteristics as they cannot resist extension, but can tolerate compression.

Let us consider a 2-D or 3-D network in which for every bond of the network the relation between q and v is given by:

$$q = g(v - v_c)^n, \; v > v_c, \tag{51}$$

$$q = 0, \; v < v_c, \tag{52}$$

where v_c is the critical voltage or threshold for the onset of transport. As in the power-law transport case, we take g to be a generalized bond conductance, which can vary from bond to bond. On the other hand, in any physical situation, such as flow of foams in porous media one expects v_c to vary from pore to pore because, for example, the threshold pressure usually depends on the shape and size of the pore. Therefore, instead of making g to be a random variable, we assume that v_c is a randomly-distributed quantity which, for the sake of simplicity, is assumed to be distributed uniformly in (0, 1), and set g to be the same for all bonds, and therefore its numerical value is irrelevant (we assume $g = 1$). The questions we ask are: what is the critical voltage V_c to have macroscopic transport in the network, and how do the macroscopic current Q and the effective conductivity g_m of the network vary with the applied voltage. The piecewise linear process that we study here is *reversible*, that is, if Q is lowered the conducting bonds become insulating again. This is an important assumption since, if we assume that the process is irreversible, then the conversion of one insulating bond to a conducting one triggers an *avalanche* effect: the conversion of the first bond makes consecutive conversions easier. Such irreversible and nonlinear models have been used to model fracture and electrical breakdown of disordered media (for a review see Sahimi, 1992b), since fracture and failure are usually irreversible processes. We should mention that Adler and Brenner (1984) investigated this problem (with fixed critical voltages) in the context of a spatially periodic capillary network model of porous media. However, such a model is perfectly ordered and contains no randomness whereas, as we showed in the previous section, it is precisely the interplay between the nonlinearity of the transport and the disordered structure of the medium that gives rise to a rich variety of behavior.

It is clear that for any applied voltage $V < V_c$ no macroscopic current can flow. Therefore, it should also be clear that

$$V_c = \min\left(\sum_i v_{ci}\right), \tag{53}$$

where v_{ci} is the critical voltage of bond i, and the sum is taken over all paths between the two terminals of the network. This immediately necessitates the concept of *minimum path* between the two terminals of the network. This concept has already been investigated for percolation clusters by Alexandrowicz (1980), Havlin and Nossal (1984), and Grassberger (1985). It was shown by these authors that for any $L << \xi$, the length $L_{\min}$ of the path scales with L as $L_{\min} \sim L^{\zeta_{\min}}$, so that $\zeta_{\min}$ can be considered as the fractal dimension of the minimum path. Currently-accepted values of this quantity are also listed in Table 1. Blumenfeld and Aharony (1985) showed that, $\zeta_{\min} = \tilde{\zeta}(n = 0^+)$, and hence this problem and that of power-law transport discussed above are actually related. Obviously, if the applied voltage is larger than some V_l, all bonds of the network will be conducting, one is in the usual linear regime, and Q is simply proportional to V. Therefore, one generally has *three* regimes of interest:

(1) If $V < V_c$, enough bonds have not become conducting to form a sample-spanning cluster, and therefore no macroscopic transport takes place. Hence, $Q = 0$, and $g_m = 0$.

(2) If $V_c < V < V_l$, then enough bonds have become conducting that they make macroscopic transport possible, while some of the bonds are still not conducting. We expect Q to depend nonlinearly on $V - V_c$, because this is precisely the regime in which the effect of nonlinearity (random voltage thresholds) should manifest itself. As we show below, this is indeed the case (note that in linear transport above p_c, Q *always* varies linearly with V).

(3) If $V > V_l$, then every bond of the network is conducting, $g_m = 1$, and Q depends linearly on V again. The fact that there is a critical threshold V_c, and that there is a regime in which Q depends nonlinearly on $V - V_c$, indicate the similarity between this problem and a percolation process. This similarity has prompted Rossen and Mamun (1993) to propose simple percolation models for this problem. However, we believe that the analogy between this problem and a percolation process is not complete, and therefore percolation alone cannot provide a quantitative description of the present problem.

We first derive an EMA for this problem, and then present our numerical results. We consider only the case $n = 1$, and generalize the continuum EMA derived by Bernasconi and Tua (1989) discussed above. They derived an EMA for this problem in a 2-D continuum with circular inclusions. We generalize it to an arbitrary network of coordination number z in 2-D or 3-D. Suppose that p is the fraction of the bonds that have become conducting, and v_{nc} is the voltage difference between the ends of the *nonconducting* bond, whose conductance is ϵ, where ϵ is very small and is eventually set to be zero. Since we assume that the critical voltages v_c are uniformly distributed in (0,1), then we must have, $dp = dv_{nc}$. Equation 14 can now be used to relate v_{nc} to V, the applied voltage. Since the transport is piecewise linear, the differential or tangent conductivity σ_m and the effective conductivity g_m are the same. Therefore, Eq. 44 becomes:

$$dv_{nc} = \frac{zg_m/2}{\epsilon + g_m(z/2 - 1)}\, dV. \tag{54}$$

But according to the EMA for linear systems we have, $g_m = 0$, if $p < 2/z$, and

$$g_m = \frac{p - 2/z}{1 - 2/z}, \; p \geq 2/z. \tag{55}$$

Thus, in the nonconducting regime we have, $dV = (1 - p)dp$, which, after integrating and using the boundary condition that $V(p = 0) = 0$, yields:

$$V = p - \frac{1}{2}p^2, \; p < 2/z. \tag{56}$$

This equation tells us how the applied voltage V varies with p *before* a sample-spanning conducting path is formed. At

$p=p_c=2/z$ the first sample-spanning conducting path is formed (remember that the problem is being treated within an EMA), at which point we have:

$$V_c=\frac{2}{z}-\frac{2}{z^2}. \tag{57}$$

For $p>2/z$ we have a conducting system, and from Eq. 54 (setting $\epsilon=0$) we obtain, $dV=[(z-2)/z]dp$, which after integrating and using the fact that $V(p=2/z)$ is given by Eq. 57, yields:

$$V=\frac{z-2}{z}p+\frac{2}{z^2},\ p\geq\frac{2}{z}. \tag{58}$$

At $p=1$ all bonds are conducting, so that the corresponding voltage is:

$$V_l=\frac{z-2}{z}+\frac{2}{z^2}. \tag{59}$$

The corresponding equations for g_m are as follows. Clearly, $g_m=0$ for $V<V_c$. For $V_c\leq V\leq V_l$ we can solve for p from Eq. 58 and substitute in Eq. 55 which yields:

$$g_m=\frac{z^2}{(z-2)^2}\left(V-\frac{2}{z^2}\right)-\frac{2}{z-2},\ V_c\leq V\leq V_l. \tag{60}$$

Obviously, $g_m=1$ for $V>V_l$.

We can now investigate the variations of Q with V. For $V<V_c$, there is no macroscopic transport and $Q=0$. Since in general, $dQ=\sigma_m dV=g_m dV$, we obtain, $dQ=[(z-2)/z][(p-2/z)/(1-2/z)]dp=(p-2/z)dp$, for $V_c\leq V\leq V_l$. If we integrate this equation, use the boundary condition that, $Q(p=2/z)=0$, and then eliminate p from the resulting equation in favor of V, we obtain:

$$Q=\frac{z^2}{2(z-2)^2}\left(V-\frac{2}{z^2}\right)^2-\frac{2}{z-2}\left(V-\frac{2}{z^2}\right)+\frac{2}{z^2},\ V_c\leq V\leq V_l. \tag{61}$$

For $V\geq V_l$, we have $g_m=1$, and we get a simple equation:

$$Q=V-\frac{1}{2}, \tag{62}$$

independent of z. Thus, our EMA predicts correctly the existence of the three transport regimes discussed above and, in particular, it predicts that for $V_c\leq V\leq V_l$, Q depends quadratically on V.

In order to test these predictions, we carried out Monte Carlo simulations of the problem using square and simple-cubic networks. The statistics of our simulations (network size, and so on) are the same as in the case of power-law transport discussed above. Figure 8 presents the variations of g_m with V in the square network. All of the qualitative features of the transport are correctly predicted by our EMA, except that our numerical

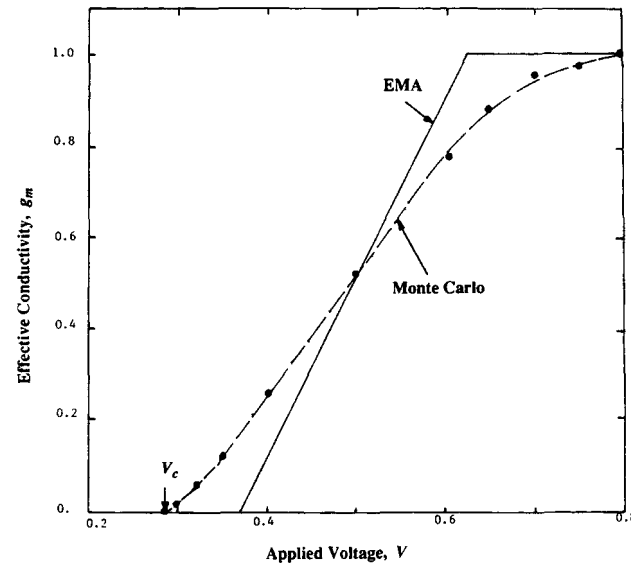

Figure 8. Variations of the effective conductivity g_m with the applied voltage V in the square network.

simulations indicate a smooth variation of g_m with V, whereas the EMA predicts a sharp transition at $V=V_l$. Figure 9 shows the variations of Q with V in the same system and, unlike the g_m case, both our numerical calculations and the EMA predict no sharp transition at $V=V_l$. However, the numerical value of V_c does not agree with the prediction of our EMA. While our Monte Carlo calculations predict, $V_c\simeq 0.29$, the EMA predicts that, $V_c=3/8=0.375$. Roux et al. (1987) used a transfer matrix method, which is a very accurate technique of estimating critical points, and estimated that for a square network, tilted at 45°, $V_c\simeq 0.23$, which is lower than ours. However, we believe that the fact that their square network was tilted makes their system somewhat different from ours, since the distribution of bond currents in their network is isotropic, whereas it is anisotropic in our network, because the bonds of our network that are perpendicular to the direction of the macroscopic

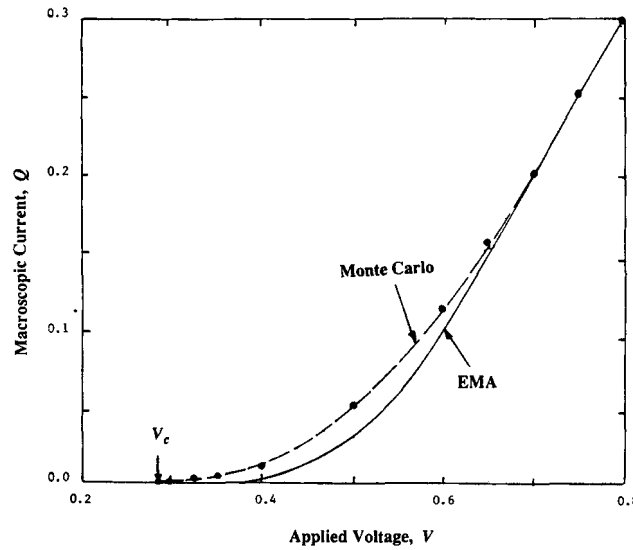

Figure 9. Variations of macroscopic current Q with the applied voltage V in the square network.

voltage drop receive much less current that those that are aligned with V. As a result, the formation of a sample-spanning cluster is easier in their system than ours, which implies that V_c of their network should be smaller than that of ours. Thus, such anisotropies, which usually have no significance for linear transport processes, are important in a nonlinear system such as what is studied here. According to Eq. 61, in the nonlinear regime, Q varies quadratically with $V - V_c$. Roux and Herrmann (1987) used accurate numerical simulations and found that, $Q \sim (V - V_c)^{\delta}$, and estimated that, $\delta \simeq 2 \pm 0.08$, in excellent agreement with our EMA prediction. Thus, as in the case of power-law transport, compared with the linear transport, the performance of the EMA has improved.

Figure 10 compares the EMA predictions with our Monte Carlo results in the cubic network, and the same qualitative trends that were seen in the square network are also observed here. We should point out that any distribution of the critical bond voltages could have been used here. We could have also selected the bond conductances g from a continuous distribution function. However, none of these would have changed the quadratic dependence of Q on $V - V_c$. On the other hand, the EMA derived above can also be extended to the case in which $n > 1$ in Eq. 51, using the technique discussed above. In this case we still expect to have a nonlinear regime, but the nonlinear dependence of Q on $V - V_c$ would be stronger than quadratic.

Nonlinear Transport due to Large Potential Gradients

In this section, we study nonlinear transport processes that arise as a result of a large external potential gradient. A large external potential gradient induces bias in the system in the sense that, in a d-dimensional system there will be an "easy" or longitudinal direction which is the direction of the external potential gradient, and along which transport takes place easier than the $(d-1)$ transverse directions. This bias also induces

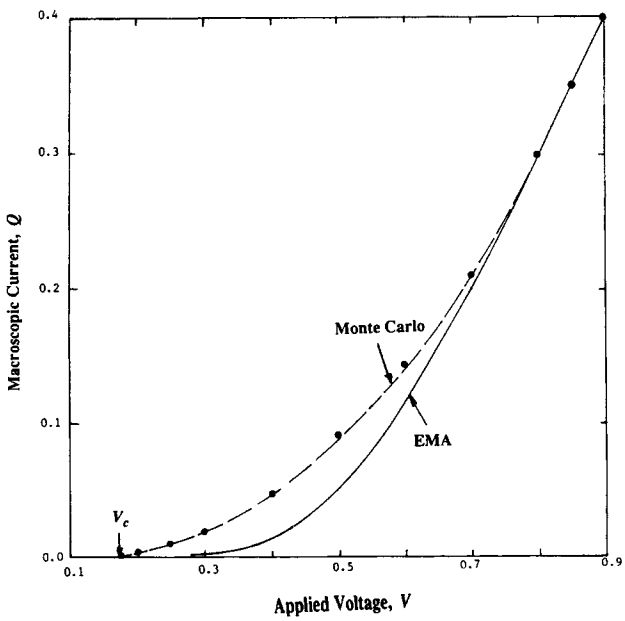

Figure 10. Variations of macroscopic current Q with the applied voltage V in the cubic network.

anisotropy in the medium such that one has to introduce *two* correlation lengths (instead of one as in isotropic systems studied above), which are the longitudinal correlation length ξ_L and the transverse correlation length ξ_T (see Figure 11). We assume that there is a critical value of the external potential V_c such that for $V > V_c$ macroscopic transport occurs. Suppose now that an external potential $V > V_c$ is imposed on the system. An example of this kind of transport is immiscible displacement processes in porous media when the strengths of capillary and viscous forces are comparable and neither of them can be neglected. Under this condition, no interface between the two immiscible fluids in any pore can be moved unless a large external pressure is applied to the system and, in general, the problem is highly nonlinear (see Sahimi, 1993a, for a review). We define a dimensionless potential $f = (V - V_c)/V_c$, which plays the same role as that of $p - p_c$ in the previous sections. Because V_c represents a kind of critical point or threshold, it is not unreasonable to assume that near $f = 0$, $\xi_L \sim f^{-\nu_L}$, and $\xi_T \sim f^{-\nu_T}$.

We should emphasize the chief difference between what we study here and that of the last section. In the present case, the

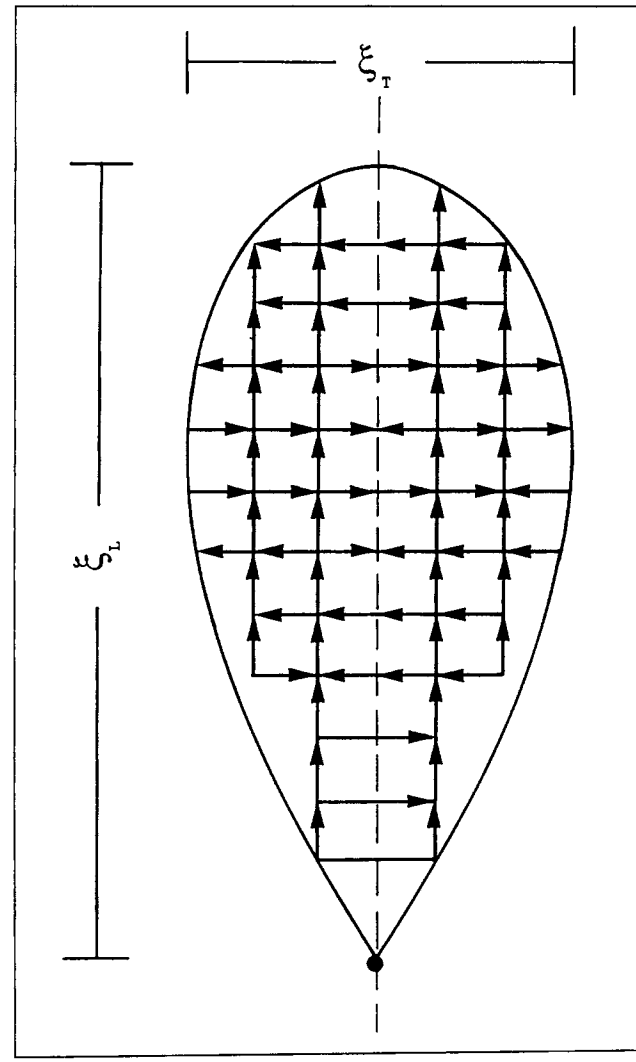

Figure 11. Strong macroscopic potential induces anisotropy in the network. ξ_L and ξ_T are the correlation lengths.

external potential is so large that it induces bias and anisotropy in the system and in the shape of the sample-spanning cluster, whereas the networks studied in the previous section remain isotropic regardless of the value of V. The problem studied here has certain similarities with *directed* percolation (for a review, see Kinzel, 1983; for more recent references, see Duarte et al., 1992). In this problem, the bonds of a percolation network are directed and diod-like. Transport along such bonds is allowed only in one direction. If the direction of the external potential is reversed, then there will be no macroscopic transport in the new direction. Similar to the present case, one also needs *two* correlation lengths to characterize the shape of directed percolation clusters. However, there is an important difference between what we study here and directed percolation. The anisotropy in our system is *dynamically* induced: if we reverse the direction of the external potential we will still have macroscopic transport, whereas the bias and anisotropy in directed percolation are *static* and fixed.

We calculate the fractal dimensions of the sample-spanning cluster and its backbone to highlight the differences between the present problem and those studied above. Transport properties of such systems will be discussed in a future article. The accessible fraction of bonds (or sites) X^A is assumed to follow a power law, $X^A \sim f^\beta$, near $f=0$. Thus, in a volume of linear dimension ξ_l, we have $X^A \sim \xi_L^{-\beta/\nu}$, and the number of sites N_s in the sample-spanning cluster is given by, $N_s \sim \xi_L \xi_T^{d-1} X^A$. Hence, if for length scales $L << \xi_L$ we define a fractal dimension for the sample-spanning cluster by $N_s \sim L^D$, then

$$D = 1 + \frac{1}{\nu_L}[\nu_T(d-1) - \beta]. \tag{63}$$

For an isotropic medium $\nu_L = \nu_T$, and Eq. 63 reduces to Eq. 3. In a similar fashion, we obtain a fractal dimension for the backbone of the cluster

$$D_B = 1 + \frac{1}{\nu_L}[\nu_T(d-1) - \beta_B], \tag{64}$$

where we made the usual assumption that the correlation length exponents are the same for the cluster and its backbone. In the absence of any numerical estimates of these critical exponents, we assume, for the moment, that the exponents ν_L, ν_T, β and β_B that we introduced here are equal to those of directed percolation. This does *not* imply that the two phenomena are the same. It only tells us that the *shapes* of conducting clusters in the two problems are roughly the same. The assumption that ν_L is the same as that of directed percolation is reasonable, because in the presence of a large external voltage V the bonds in the longitudinal direction essentially have the same configuration as those in directed percolation. However, the situation in the transverse direction is somewhat more complex and shall be discussed shortly.

For directed percolation one has, $\nu_L \simeq 1.734$ and 1.27, $\nu_T \simeq 1.1$ and 0.735, $\beta \simeq 0.28$ and 0.6, and $\beta_B = 2\beta$, for $d=2$ and 3, respectively. Thus, we obtain $D \simeq 1.47$ and 1.68, and $D_B \simeq 1.31$ and 1.21, for $d=2$ and 3, respectively. For a Bethe network, we have, $\nu_L = 1$, $\nu_T = 1/2$, $\beta = 1$ and $\beta_B = 2$, which imply that $D=2$ and $D_B = 1$. Two points are worth mentioning here. First of all, the values of D imply that a large external field and the associated dynamical bias and anisotropy give rise to conducting clusters with low fractal dimensions. This can be understood by noting that, in such systems transport is essentially restricted to a narrow cone (see Figure 11). Secondly, the fractal dimensions D and D_B calculated here are considerably smaller than those of isotropic percolation (see Table 1) and, in particular, unlike D_B for isotropic percolation, Eq. 64 predicts that D_B *decreases* as d increases. This can be understood if we consider the problem on the Bethe network. In this case, any large external potential makes the network completely directed, since there are no closed loops. As a result, the backbone is made of directed branches which have a quasi-one-dimensional structure, and thus $D_B = 1$.

To improve upon these results and obtain more realistic estimates for D and D_B we proceed as follows. Any given event in which a bond becomes conducting is independent of all other bonds. Therefore, the transverse bonds become conducting completely at random (because the mean voltage fluctuations in the transverse direction is zero), and the overall process is a random walk. That is, we can imagine that the consecutive events in which bonds become conducting are in fact consecutive steps of a random walk in $(d-1)$ transverse directions. If so, we should have $\xi_T \sim \xi_L^{1/2}$, that is, the longitudinal direction acts as the time axis, and therefore the distance that the random walker travels in the transverse direction should increase with the square root of time (which is the law of random walks or ordinary diffusion). This implies that $\nu_T = \nu_L/2$, and therefore

$$D = \frac{d+1}{2} - \frac{\beta}{\nu_L}, \tag{65}$$

and

$$D_B = \frac{d+1}{2} - \frac{\beta_B}{\nu_L}. \tag{66}$$

We thus obtain $D \simeq 1.34$ and 1.53, and $D_B \simeq 1.18$ and 1.06, for $d=2$ and 3, respectively. These values are even smaller than what we obtained above, and represent more accurate estimates of the true values of D and D_B.

Nonlinear Transport in Disordered Continua

So far we have used random conductance networks as the model of a disordered medium. We now consider power-law transport and discuss how our results may change if we use a continuum model. The most notable differences between the two cases are in the scaling behavior of the transport properties near p_c, and therefore we only discuss this aspect of the problem. It is almost always possible to map a disordered continuum onto an equivalent network, an example of which was discussed in the Introduction. However, if we use the equivalent network, instead of the continuum itself, we should also decorate the network with the natural distribution of the conductances. Moreover, not only should we select the bond conductances from the natural distribution, we should also make sure that the correlations that usually exist in a continuum are not destroyed. Such correlations, which are between the conductance of the neighboring bonds, are usually of short range, and it is generally believed that they do not change the scaling properties of a given system, so that the critical exponents remain

unchanged, although the numerical value of a given property in a correlated system may be quite different from that of a completely random one.

However, depending on the structure of the natural distribution, the scaling properties of the *transport properties* can change. Consider first the case of a linear transport process, such as conduction or diffusion, in a disordered continuum, such as that shown in Figure 2. It was shown by Feng et al. (1987) that the scaling of the transport properties of this system near its percolation threshold is very different from those of a random network. In particular, if t_{sc} denotes the critical exponent of the conductivity of the system, then for a 3-D Swiss-Cheese model one has (Feng et al., 1987)

$$t_{sc} \simeq t + \frac{1}{2}. \tag{67}$$

Moreover, one has to define a *permeability* exponent which, unlike the case of random networks, is very different from the conductivity exponent t. If, near p_c, the permeability k of the system obeys the scaling law, $k \sim (p - p_c)^{e_{sc}}$, then (Feng et al., 1987)

$$e_{sc} \simeq t + \frac{3}{2}, \tag{68}$$

for 2-D systems, and

$$e_{sc} \simeq t + \frac{5}{2}, \tag{69}$$

for 3-D systems. These equations imply that near p_c the permeability curves of the Swiss-Cheese systems are much flatter than those of random networks. To obtain an estimate of conductivity exponent for power-law transport in the Swiss-Cheese system we proceed as follows. Since, as we showed above, the exponent $\zeta(n)$ depends only weakly on n, we assume that it is approximately constant. Equation 67 would then imply that, $\zeta_{sc} = \zeta + 1/2$, where ζ_{sc} is the analog of ζ for the Swiss-Cheese model. This would then imply that:

$$t_{sc}(n) \simeq (d-1)\nu + \frac{\zeta + 1/2 - \nu}{n} = t(n) + \frac{1}{2n}, \tag{70}$$

which reduces to Eq. 67 in the limit $n = 1$. We can use the same argument to obtain an estimate of the permeability exponent $e_{sc}(n)$. Thus, for a 3-D Swiss-cheese system we obtain:

$$e_{sc}(n) \simeq t(n) + \frac{5}{2n}, \tag{71}$$

which reduces to Eq. 69 in the limit $n = 1$. Equations 70 and 71 should provide reasonable estimates of $e_{sc}(n)$ and $t_{sc}(n)$. They also show that the permeability and conductivity curves for power-law transport in a continuum are much flatter than those of random networks. It was also shown by Straley (1982) and Feng et al. (1987) that if the conductance distribution of a random continuum is of the form, $f(g) = (1-p)\delta(g) + p(1-\alpha)g^{-\alpha}$, where $0 \le \alpha \le 1$, then the conductivity critical exponent $t(\alpha)$ of this system is *not* universal and is given by:

$$t_l(\alpha) = 1 + (d-2)\nu + \frac{\alpha}{1-\alpha} \le t(\alpha) \le t + \frac{1}{1-\alpha}. \tag{72}$$

Thus, using the same technique and assumption as the above, we may obtain an estimate for $t(\alpha, n)$ or $e(\alpha, n)$ for power-law transport in such a continuum. Feng et al. (1987) showed that such power-law conductance distributions are very common among disordered continua. In fact, for the Swiss-Cheese models in d-dimensions one has, $\alpha = (2d-5)/(2d-3)$. In $d = 2$, $\alpha = -1$, and the distribution is not singular at $g = 0$, and therefore $t_{sc} = t$. In $d = 3$, $\alpha = 1/3$, and the conductance distribution is singular at $g = 0$, and gives rise to Eq. 67. Moreover, Straley (1982) argued that:

$$t(\alpha) = \min[t,\ t_l(\alpha)]. \tag{73}$$

Sahimi et al. (1983a) showed that such singular distributions can give rise to unusual diffusion phenomena, including one in which the mean square displacement of a diffusing particle grows with time slower than linearly, and the long-time diffusivity is zero. Note that such power-law conductance distributions do not obey (Eq. 8), which explains the nonuniversality of $t(\alpha)$.

A few points are worth mentioning here. First of all, the above exponents for a continuum can also be obtained with the network models if we select the bond conductances from the natural distribution of the continuum. Thus, our analysis of power-law transport in a Bethe network remains completely valid. All we have to do is to use a distribution $f(g)$ which corresponds to that of a continuum. Secondly, if we want to use Eqs. 34 and 35 for power-law fluid flow in a continuum, we should replace t_n with its corresponding value for a continuum (for example, Eq. 70). Finally, we can convert Eqs. 47 and 48 to EMAs for disordered continua by converting $2/z$ and the exponent $1/n$ to their corresponding values for a continuum. For example, for the Swiss-Cheese model, we should replace $2/z$ with $1/d$, and the exponent $1/n$ with $3/2n$, so that Eq. 47 may be rewritten as:

$$g_m = \left[\frac{(pd)^n - 1}{d^n - 1}\right]^{3/2n}. \tag{74}$$

These results demonstrate the subtle differences between random network models and disordered continua.

Summary

Using percolation and scaling concepts, effective-medium approximation, and Monte Carlo simulations, we studied three types of nonlinear transport processes in disordered media. Our results clearly demonstrate that the interplay between the disordered structure of the media and the nonlinear nature of the transport process can give rise to a rich variety of macroscopic transport regimes that are completely absent in linear systems. One surprising result was that the effective-medium approximations for the nonlinear systems that we studied turned out to be more accurate than those for linear systems.

Many of our results can be generalized to more complex nonlinear transport in random media. For example, if the

relation between q and v is of the form, $q=f_1(v)$, where f_1 is any physically-acceptable function of v, we can approximate f_1 by several straight lines and obtain a system characterized by *several* thresholds, each one of which would describe the transition from one linear relation between q and v to another one. The EMA developed in Section 4 can then be generalized to describe the $Q-V$ behavior of such systems. Stroud and Hui (1988) and Zeng et al. (1988) have studied the effective dielectric function of a heterogeneous solid in which there is a weakly nonlinear relation between electric displacement $\boldsymbol{D}$ and electric field $\boldsymbol{E}$ of the form $\boldsymbol{D}=\epsilon\boldsymbol{E}+\chi|\boldsymbol{E}|^2\boldsymbol{E}$, where ϵ and χ are random variables. Likewise, we can study random networks in which transport in a fraction of the bonds is linear, but it is nonlinear in the rest of the bonds, and it is of the form, $q=gv+\chi v^{\alpha}$, with $\alpha>1$. This would enable us to study the so-called Frocheimer regime of fluid flow which is the limit $\alpha=2$. In such cases we may expect to obtain an even richer variety of macroscopic transport phenomena than what we studied in this article. We hope that our results will stimulate more work in this rich and important area of research.

Acknowledgment

The author is grateful to Yanis Yortsos for pointing out the possibility of extending the critical path analysis to power-law transport and to Jacob Bernasconi and Bill Rossen for sending him their unpublished works. This article was prepared while the author was visiting the HLRZ Supercomputer Center as an Alexander von Humboldt Foundation Research Fellow. He is grateful to the Center and Hans Herrmann for warm hospitality and to the Foundation for financial support.

Notation

d = Euclidean dimensionality
D = fractal dimension of the sample-spanning cluster
D_B = fractal dimension of the backbone
e_{sc} = permeability exponent of Swiss-cheese model
$\mathbf{E}$ = electric field
f = conductance distribution
F = formation factor
g = bond conductance
g_m = effective conductivity of a network
G = conductance of a branch of a Bethe network
G_m = effective conductance of a branch of a Bethe network
h = conductance distribution
H = conductance distribution of a branch of a Bethe network
I = dissipated power
k = effective permeability
l = pore length
l_c = critical length scale
L = network size
m = parameter of power-law fluids
M_{red} = number of red bonds
n = power-law exponent
p = fraction of conducting bonds
p_c = percolation threshold
P = pressure
q = microscopic current
Q = macroscopic current
r = bond resistance
R = blob resistance
R_t = tube radius
S = surface area
t = conductivity exponent
t_n = power-law conductivity exponent
t_{sc} = swiss-cheese conductivity exponent
u_m = mean flow velocity
v = microscopic voltage
v_c = microscopic critical voltage
V = macroscopic voltage
V_c = macroscopic critical voltage
X^A = accessible fraction
X^B = backbone fraction
z = coordination number

Greek letters

α = parameter of conductance distribution
β = exponent of accessible fraction
β_B = exponent of backbone fraction
ξ = correlation length
ξ_L = longitudinal correlation length
ξ_T = transverse correlation length
ζ = resistivity exponent
ζ_{min} = fractal dimension of minimum paths
ζ_{red} = fractal dimension of the red bonds
λ = Laplace transform variable
ν = correlation length exponent
ν_L = longitudinal correlation length exponent
ν_T = transverse correlation length exponent
ϕ = porosity
σ = tangent conductance
σ_m = effective tangent conductivity

Literature Cited

Adler, P. M., and H. Brenner, "Transport Processes in Spatially Periodic Capillary Networks: III. Nonlinear Flow Problems," *PhysicoChem. Hydrodyn.*, **5**, 287 (1984).

Alexandrowicz, Z., "Critically Branched Chains and Percolation Clusters," *Phys. Lett.*, **A80**, 284 (1980).

Ambegaokar, V., B. I. Halperin, and J. S. Langer, "Hopping Conductivity in Disordered Systems," *Phys. Rev.*, **B4**, 2612 (1971).

Arbabi, S., and M. Sahimi, "Test of Universality for Three-Dimensional Models of Mechanical Breakdown in Disordered Solids," *Phys. Rev.*, **B41**, 772 (1990).

Benzoni, J., and H.-C. Chang, "Effective Diffusion in *Bi*-Disperse Media—an Effective Medium Approach," *Chem. Eng. Sci.*, **39**, 161 (1984).

Bernasconi, J., and P. F. Tua, Brown Boveri Research Report, unpublished (1989).

Bird, R. B., R. C. Armstrong, and O. Hasseger, *Dynamics of Polymeric Liquids*, 2nd Ed., Wiley, New York (1987).

Blumenfeld, R., and A. Aharony, "Nonlinear Resistor Fractal Networks, Topological Distances, Singly Connected Bonds and Fluctuations," *J. Phys. A*, **18**, L443 (1985).

Blumenfeld, R., Y. Meir, A. B. Harris, and A. Aharony, "Infinite Set of Exponents for Describing Physics on Fractals," *J. Phys. A*, **19**, L791 (1986).

Bruggeman, D. A. G., "Berechueng Verschiedener Physikalischer Konstanten von Heterogenen Substanzen: I. Dieletrizitatskoustanten und Leitfahigkeiten der Mischkorper aus Isotropen Substanzen," *Ann. Phys.*, **24**, 636 (1935).

Burganos, V. N., and A. C. Payatakes, "Knudsen Diffusion in Random and Correlated Networks of Constricted Pores," *Chem. Eng. Sci.*, **47**, 1383 (1992).

Burganos, V. N., and S. V. Sotirchos, "Diffusion in Pore Networks: Effective Medium Theory and Smooth Field Approximation," *AIChE J.*, **33**, 1678 (1987).

Cannella, W. J., C. Huh, and R. S. Seright, "Prediction of Xanthan Rheology in Porous Media," SPE 18089, Houston (1988).

Chauveteau, G., and A. Zaitoun, "Basic Rheological Behavior of Xanthan Polysaccharide Solutions in Porous Media: Effects of Pore Size and Polymer Concentration," *Proc. Eur. Symp. Enhanced Oil Recovery*, p. 197, F. J. Fayers, ed. (1981).

Christopher, R. H., and S. Middleman, "Power-Law Flow Through Porous Media," *Ind. Eng. Chem. Fund.*, **4**, 422 (1965).

Coniglio, A., "Thermal Phase Transition of the Dilute *s*-State Potts and *n*-Vector Models at the Percolation Threshold," *Phys. Rev. Lett.*, **46**, 250 (1981).

Duarte, J. A. M. S., J. M. Carvalho, and H. J. Ruskin, "The Direction of Maximum Spread in Anisotropic Forest Fires and its Critical Properties," *Physica*, **A183**, 411 (1992).

Duda, J. L., S. A. Hong, and E. E. Klaus, "Flow of Polymer Solutions

in Porous Media: Inadequacy of the Capillary Model," *Ind. Eng. Chem. Fund.*, **22**, 299 (1983).
Feng, S., B. I. Halperin, and P. N. Sen, "Transport Properties of Continuum Systems near the Percolation Threshold," *Phys. Rev.*, **B35**, 197 (1987).
Gogarty, W. B., "Rheological Properties of Pseudo-plastic Fluids in Porous Media," *Soc. Pet. Eng. J.*, **7**, 149 (1967).
Grassberger, P., "On the Spreading of Two-dimensional Percolation," *J. Phys. A*, **18**, L215 (1985).
Havlin, S., and R. Nossal, "Topological Properties of Percolation Clusters," *J. Phys. A*, **17**, L427 (1984).
Heiba, A. A., M. Sahimi, L. E. Scriven, and H. T. Davis, "Percolation Theory of Two-Phase Relative Permeability," SPE 11015, New Orleans, LA (1982).
Heinrichs, J., and N. Kumar, "Simple Exact Treatment of Conductance in a Random Bethe Lattice," *J. Phys. C*, **8**, L510 (1975).
Hirasaki, G. J., and G. A. Pope, "Analysis of Factors Influencing Mobility and Adsorption in the Flow of Polymer Solution through Porous Media," *Soc. Pet. Eng. J.*, **14**, 337 (1974).
Jerauld, G. R., L. E. Scriven, and H. T. Davis, "Percolation and Conduction on the 3D Voronoi and Regular Networks: A Second Case Study in Topological Disorder," *J. Phys. C*, **17**, 3429 (1984).
Katz, A. J., and A. H. Thompson, "Quantitative Prediction of Permeability in Porous Media," *Phys. Rev.*, **B34**, 8179 (1986).
Katz, A. J., and A. H. Thompson, "Prediction of Rock Electrical Conductivity from Mercury Injection Measurements," *J. Geophys. Res.*, **B92**, 599 (1987).
Kenkel, S. W., and J. P. Straley, "Percolation Theory of Nonlinear Circuit Elements," *Phys. Rev. Lett.*, **49**, 767 (1982).
Kerstein, A. R., "Equivalence of the Void Percolation Problem for Overlapping Spheres and a Network Problem," *J. Phys. A*, **16**, 3071 (1983).
Kinzel, W., "Percolation Structures and Processes," *Ann. Israel Phys. Soc.*, **5**, 425 (1983).
Kirkpatrick, S., "Percolation and Conduction," *Rev. Mod. Phys.*, **45**, 574 (1973).
Koplik, J., "On the Effective Medium Theory of Random Linear Networks," *J. Phys. C*, **14**, 4821 (1981).
Landauer, R., "The Electrical Resistance of a Binary Mixture," *J. Appl. Phys.*, **23**, 779 (1952).
Landauer, R., "Electrical Transport and Optical Properties of Inhomogeneous Media," *AIP Conf. Proc.*, **40**, 2 (1978).
Larson, R. G., "Derivation of Generalized Darcy Equations for Creeping Flow in Porous Media," *Ind. Eng. Chem. Fund.*, **20**, 132 (1981).
Marshall, R. J., and A. B. Metzner, "Flow of Viscoelastic Fluids Through Porous Media," *Ind. Eng. Chem. Fund.*, **6**, 393 (1967).
Meir, Y., R. Blumenfeld, A. Aharony, and A. B. Harris, "Series Analysis of Randomly Diluted Nonlinear Resistor Networks," *Phys. Rev.*, **B34**, 3424 (1986).
Moukarzel, C., and H. J. Herrmann, "A Vectorizable Random Lattice," *J. Stat. Phys.*, **68**, 911 (1992).
Odeh, A. S., and H. T. Yang, "Flow of Non-Newtonian Power-Law Fluids Through Porous Media," *Soc. Pet. Eng. J.*, **19**, 155 (1979).
Rossen, W. R., and C. K. Mamun, "Minimal Path for Transport in Networks," *Phys. Rev.*, submitted (1993).
Roux, S., A. Hansen, and E. Guyon, "Criticality in Non-linear Transport Properties of Heterogeneous Materials," *J. Physique*, **48**, 2125 (1987).
Roux, S., and H. J. Herrmann, "Disorder-Induced Nonlinear Conductivity," *Europhys. Lett.*, **4**, 1227 (1987).
Sahimi, M., "On the Determination of Transport Properties of Disordered Systems," *Chem. Eng. Commun.*, **64**, 177 (1988).
Sahimi, M., "Transport of Macromolecules in Porous Media," *J. Chem. Phys.*, **96**, 4718 (1992a).
Sahimi, M., "Brittle Fracture in Disordered Systems: From Reservoir Rocks to Composite Solids," *Physica*, **A186**, 160 (1992b).
Sahimi, M., "Flow Phenomena in Rocks: From Continuum Models to Fractals, Percolation, Cellular Automata and Simulated Annealing," *Rev. Mod. Phys.*, to be published (1993a).
Sahimi, M., *Applications of Percolation Theory*, Taylor and Francis, London (1993b).
Sahimi, M., and S. Arbabi, "Percolation and Fracture in Disordered Solids and Granular Media: Approach to a Fixed Point," *Phys. Rev. Lett.*, **68**, 608 (1992).
Sahimi, M., G. R. Gavalas, and T. T. Tsotsis, "Statistical and Continuum Models of Fluid-Solid Reactions in Porous Media," *Chem. Eng. Sci.*, **45**, 1443 (1990).
Sahimi, M., and J. D. Goddard, "Elastic Percolation Models for Cohesive Mechanical Failure in Hetergeneous Systems," *Phys. Rev.*, **33**, 7848 (1986).
Sahimi, M., B. D. Hughes, L. E. Scriven, and H. T. Davis, "Stochastic Transport in Disordered Systems," *J. Chem. Phys.*, **78**, 6849 (1983a).
Sahimi, M., B. D. Hughes, L. E. Scriven, and H. T. Davis, "Real-Space Renormalization and Effective Medium Approximation to the Percolation Conduction Problem," *Phys. Rev.*, **B28**, 307 (1983b).
Savins, J. G., "Non-Newtonian Flow Through Porous Media," *Ind. Eng. Chem.*, **61**, 81 (1969).
Scheidegger, A. E., *The Physics of Flow Through Porous Media*, 3rd ed., Univ. of Toronto Press, Toronto (1974).
Sheffield, R. E., and A. B. Metzner, "Flows of Nonlinear Fluids Through Porous Media," *AIChE J.*, **22**, 736 (1976).
Sorbie, K. S., and P. J. Clifford, and E. R. W. Jones, "The Rheology of Pseudoplastic Fluids in Porous Media Using Network Modeling," *J. Colloid Interface Sci.*, **130**, 508 (1989).
Stanley, H. E., "Cluster Shapes at the Percolation Threshold: An Effective Cluster Dimensionality and its Connection with Critical-Point Exponents," *J. Phys*, **A11**, L211 (1977).
Stauffer, D., and A. Aharony, *Introduction to Percolation Theory*, 2nd ed., Taylor and Francis, London (1992).
Stinchcombe, R. B., "Conductivity and Spin-Wave Stiffness in Disordered Systems-an Exactly Soluble Model," *J. Phys.*, **C7**, 179 (1974).
Straley, J. P., "Random Resistor Tree in an Applied Field," *J. Phys.*, **C10**, 3009 (1977).
Straley, J. P., "Non-universal Threshold Behavior of Random Resistor Networks with Anomalous Distributions of Conductances," *J. Phys.*, **C15**, 2343 (1982).
Straley, J. P., and S. W. Kenkel, "Percolation Theory for Nonlinear Conductors," *Phys. Rev.*, **B29**, 6299 (1984).
Stroud, D., and P. M. Hui, "Nonlinear Susceptibilities of Granular Matter," *Phys. Rev.*, **B37**, 8719 (1988).
Tua, P. F., and J. Bernasconi, "Monte Carlo Simulations of Two-dimensional Randomly Diluted Networks of Nonlinear Resistors," *Phys. Rev.*, **B37**, 1986 (1988).
Teeuw, D., and F. T. Hesselink, "Power-Law Flow and Hydrodynamic Behavior of Biopolymer Solutions in Porous Media," SPE 8982, Stanford Univ. (1980).
Thorpe, M. F., and P. N. Sen, "Elastic Moduli of Two-dimensional Composite Continua with Elliptical Inclusions," *J. Accoust. Soc. Amer.*, **77**, 1674 (1985).
Wu, Y.-S., K. Pruess, and P. A. Witherspoon, "Displacement of a Newtonian Fluid by a Non-Newtonian Fluid in a Porous Medium," *Transp. Porous Media*, **6**, 115 (1991).
Zeng, X. C., D. J. Bergman, P. M. Hui, and D. Stroud, "Effective-Medium Theory for Weakly Nonlinear Composites," *Phys. Rev.*, **B38**, 10970 (1988).

Manuscript received June 26, 1992, and revision received Dec. 16, 1992.